Networked Hydrographical Systems: A Reactive Control Strategy Integrating Time Transfer Delays

Eric Duviella[1], Pascale Chiron[2], Philippe Charbonnaud[2]

[1] Ecole des Mines de Douai, Département Informatique et Automatique

941, rue Charles Bourseul, BP 10838, 59508 Douai Cedex, France,

E-mail: duviella@ensm-douai.fr

[2] Laboratoire Génie de Production

ENIT, 47 av. d'Azereix, BP 1629

65016 Tarbes Cedex, France

E-mail: pascale.chiron@enit.fr, philippe.charbonnaud@enit.fr

Abstract: A reactive control strategy integrating time transfer delays is proposed to improve the water-asset management of networked hydrographical systems. The considered systems are characterized by large scale networks where each diffluence is equipped with a control gate and a measurement point. Modelling methods of the networked hydrographical systems with equipped diffluences are presented. The proposed strategy, based on a supervision and hybrid control accommodation approach, requires generic resource allocation and setpoint assignment rules. The simulation results show the effectiveness of the reactive control strategy.

Keywords: supervision, hybrid control accommodation, resource allocation, setpoint assignment, gridded systems, water management.

Eric Duviella was born in France in 1978. Since 2007, he is assistant professor in the Computer Sciences and Automatic Department of the Ecole des Mines de Douai, France. In 2005, he has obtained his Ph.D degree from the Institut National Polytechnique de Toulouse on 'Reactive control of extended dynamic systems with variable time delays - Application to hydrographic networks'. His research interests include modelling, hybrid dynamical systems, supervision, reactive control strategy.

Pascale Chiron was born in France in 1961. She is assistant professor (Maître de conférences) at ENIT (National School of Engineers in Tarbes) since 2000. She has obtained her Ph.D in 1989 at Ecole Centrale in Nantes on « matching and similarity criterion in medical imaging ». She was a postdoctoral fellow at Radiology and nuclear medicine department, Faculty of medicine, Kyoto University, Japan from 1989 to 1990. Now, she is involved in theme « Planning, Control, Supervision and Distributed Simulation» in the « Automated Production » Group of Laboratoire de Génie de Production at ENIT. Her domains of interest are modelling and simulation for system control.

Philippe Charbonnaud was born in 1962 at Angoulême, France and received his Ph.D graduation in 1991 from the University Bordeaux 1. Since 2002, he is graduated Hd.R (Habilitation à diriger les Recherches) from Institut National Polytechnique de Toulouse. Since 2003, he fas been Full Professor at Ecole Nationale d'Ingénieurs de Tarbes. He is member of the IFAC TC 5.4 on Large Scale Control System. His main topic of interest concerns the real-time decision support systems, and more particularly supervision and control accommodation of distributed systems.

1. Introduction

Hydrographical system is a geographically distributed network composed of dams and interconnected rivers and channels. It is characterized by great dimensions and composed of confluences and diffluences. In real case, each diffluence is very often equipped with a control gate and a measurement point. The flow discharges are greatly disturbed by the human activities and weather conditions. An interesting problem to address, deals with the allocation of water quantities in excess toward the catchment's areas and of water quantities in lack amongst the users. The representations of networked hydrographical systems with equipped diffluences, as well as the determination of the discharge allocation on the network, are an essential step for the design of reactive control strategy. In [18], a hydrographical network representation considering only the diffluences is proposed. Indexed nodes represent the points of diffluence, and directed arcs, whose indexes represent the number of the node downstream, represent the hydrographical systems that connect two nodes. This model was modified and extended to the case of the confluences in [13]. In these approaches, the control and measurement instrumentations are not taken into account. In [4, 15], object-oriented modelling techniques and a XML approach make it possible to represent the elements of the hydrographical networks and of the drinking water distribution networks. Finally, modelling approaches are proposed for the optimal water management of the irrigation networks in [17], of the drinking water distribution networks, and of sewerage networks in [3]. For these four last approaches, the representation of the control and measurement instrumentations allows integrating computation rules of the

discharge propagation upstream to downstream, but these rules are not adapted with the water-asset management optimization goal.

Optimization techniques were proposed in the literature for the water-asset management. The approach proposed in [10] allows the adjustment of the criteria and the constraints of an optimization problem starting from the supervision of the network variables. However, the complexity of the hydrographical networks and the number of the instrumented points to be taken into account in the optimization problem require the use of decomposition and coordination techniques of the studied systems as proposed in [17]. These techniques are used for the optimal water management of irrigation systems. In addition, a supervision and hybrid control accommodation strategy is proposed in [9] for the water-asset management of the Neste canal located in the south western region of France. This strategy is successfully adapted for the case of dam-river networks that are characterized by non-equipped diffluences [7]. Finally, to take into account majority of the networked hydrographical systems, the supervision and hybrid control accommodation strategy has to be adapted for the case of diffluences equipped with a control gate and a measurement point.

In this paper, the water asset-management by resource allocation and setpoint assignment is considered. Hydrographical systems with confluences and equipped diffluences and their representation by a weighted digraph are presented in section 2. In section 3, the reactive control strategy is defined for the water-asset management of these systems. Finally, the effectiveness of the proposed strategy is shown by simulation within the framework of a networked hydrographical system that is part of a real network. This system is composed of two diffluences and one confluence, and supplies with water downstream dams.

2. Modelling Steps of Networked Hydrographical Systems with Equipped Diffluences

Networked hydrographical systems are composed of dams and interconnected rivers and channels. The river and channels are constituted of a finite number of *Simple* Hydrographical Systems (HYS), *i.e.* composed of one stream. A representation is proposed to be able to highlight the links between the rivers, the channels and the dams, and to locate the instrumentation, *i.e.* the measurement points and controlled gates (*see* Figure 1.*a* and *b*). Each hydrographical system is equipped with several measurement points M_i and controlled gates G_j, with $i \in [1, m]$ and $j \in [1, n]$, where m and n are respectively the total number of measurement points and actuators. It is assumed that each diffluence is equipped with at least a control gate and a measurement point. To determine the way to distribute a water quantity measured in a place of the hydrographical network, onto the whole system downstream, the networked system is represented by a digraph of instrumented points (*see* Figure 1.*c* and *d*).

Step 1. A digraph of instrumented points is proposed to describe the structure of the networked system by distinguishing the confluence (*see* Figure 1.*a* and *c*) and the diffluence (*see* Figure 1.*b* and *d*). The digraph consists of a succession of two types of nodes M_i and G_j, represented respectively by full circle and circle and their associated graphs, and two types of arcs $L_S^{d,c}$ and $L_D^{d,c}$ represented respectively by solid and dashed line, which show the links between the successive nodes d and c and the direction of the flow (*see* Figure 1.*c* and *d*). The attribute of the arc L is D in the case of a diffluence, and S otherwise.

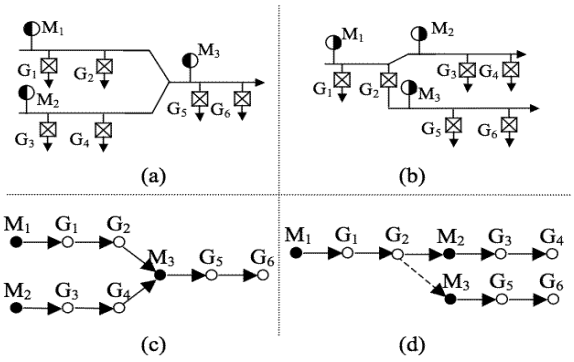

Figure 1. (*a*) A confluence, (*c*) its associated weighted digraph, (*b*) a diffluence, (*d*) its associated weighted digraph**.**

Thereafter, in order to represent the possible influence of measurement points, the matrix **R** composed of *m* lines (measurement points) and of *n* columns (actuators), is generated. The digraph is browsed for each measurement point M_i following the algorithm given in Table I. The proposed algorithm, a classical depth-first search like algorithm [6], has not been optimized in term of numerical complexity. The algorithm is only used during the design steps of the reactive control strategy and thus numerical complexity is not a challenge. The value of $R(i, j)$ is equal to 1 if there is a direct path between the measurement point M_i and the gate G_j, and 0 otherwise. A direct path from M_i to G_j, is a path where no arc L_D can be met between M_i and G_j.

TABLE I. Assignment function of R matrix**.**

```
Input: digraph.
Output: proportion matrix R.
Initialisation of R to 0
For each node h
If h is a measurement point
    Run (h, h, R)
EndIf
EndFor

Run (h, c, R),
For each successor d of c
    If L^{c,d} is L_S
        Run (h, d, R)
    EndIf
    If d is a gate
        R(h, d) ← 1
    EndIf
EndFor
```

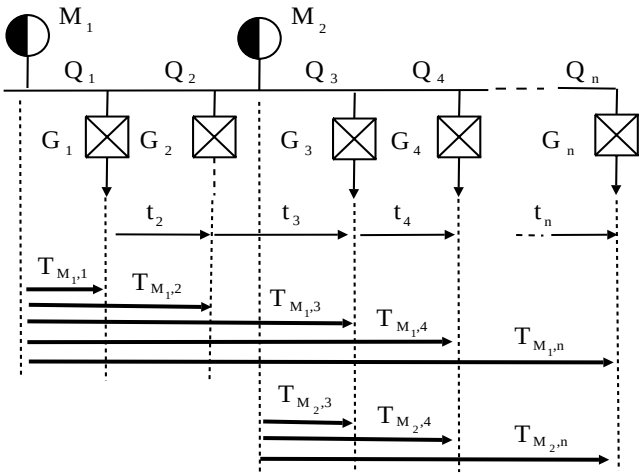

Figure 2. Time delays between measurement points and gates.

Step 2. The value of the transfer time delay $T_{M_i,j}$ between the measurement point M_i and the gate G_j are computed only if a direct path exists between M_i and G_j, *i.e.* $R(i, j) = 1$. Open-Channel Reach Section (OCRS) is a part of HYS defined between a measurement point and a gate, between a gate and a measurement point, or between two gates. The transfer delay $T_{M_i,j}$ between the measurement point M_i and the gate G_j (*see* Figure 2) can be calculated by the relation:

$$T_{M_i,j} = T_{M_i,n_i} + \delta^1_{R(i,j)} \sum_{g=n_i+1}^{j} t_g, \tag{1}$$

with $n_i + 1 \le j \le n$, where n_i is the index of the first gate downstream the measurement point M_i, n the total number of gates, and δ^b_a is the Kronecker index, equal to 1 when $a = b$, and equal to 0 otherwise. The trans-

fer delay t_g associated to each OCRS is computed from the OCRS dynamics model described thereafter.

Usually, Saint Venant equations are used for the modelling of open channel dynamics. The analytic resolution of these two-coupled partial differential equations [5] is not possible. As discussed in [14, 1] discretisation methods can be used to find a solution. Otherwise, a modelling method detailed in [16] based on the simplification and linearization of Saint Venant equations can be used. This method is based on the identification for each OCRS of a transfer function plus transfer delay (2) for a reference discharge Q_e [8], according to the OCRS geometrical characteristics.

$$F(s) = \frac{e^{-\tau s}}{1 + w_1 s + w_2 s^2}, \tag{2}$$

where the coefficients *w1*, *w2* and the pure delay τ are computed according to the identified celerity and diffusion parameters C_e and D_e, and to the adimensional coefficient C_L which is defined by:

$$C_L = \frac{2C_e X}{9D_e}, \tag{3}$$

where X is the OCRS length, C_e and D_e are expressed as:

$$\begin{cases} C_e = \dfrac{1}{L^2}\dfrac{\partial J}{\partial Q_e}\left[\dfrac{\partial L}{\partial x} - \dfrac{\partial JL}{\partial y}\right], \\ D_e = \dfrac{1}{L\dfrac{\partial J}{\partial Q_e}}, \end{cases} \tag{4}$$

where L is the surface width, y the discharge depth, J the friction slope expressed with the Manning-Strickler relation as $J = \dfrac{Q_e^2 P^{\frac{4}{3}}}{K^2 S^{\frac{10}{3}}}$, where K is the Strickler coefficient, P the wetted perimeter and S the wetted surface.

As displayed in Table II, the order of the transfer function depends on the C_L value. When $C_L \le \frac{4}{9}$, the OCRS is short and can be modelled by a first order transfer function without delay, when $\frac{4}{9} < C_L \le 1$, a delay is added to a first order transfer function and when $C_L > 1$, the OCRS is long enough and can be modelled by a second order transfer function with delay.

TABLE II. Continuous transfer functions *F(s)* corresponding to *CL*.

C_L	$F(s)$
$C_L \le \frac{4}{9}$	$F(s) = \dfrac{1}{1 + w_1 s}$
$\frac{4}{9} < C_L \le 1$	$F(s) = \dfrac{e^{-\tau s}}{1 + w_1 s}$
$C_L > 1$	$F(s) = \dfrac{e^{-\tau s}}{1 + w_1 s + w_2 s^2}$

The time delay t_g (*see* relation (1)) depends on the network configuration (the followed path). It is computed from the step response of the transfer function, which is identified around the reference discharge Q_e, and corresponds to the time so that 50% of the step response is reached. Then, the transfer delay $T_{M_i,j}$ (1) is expressed according to the sampling period T_s:

$$kd_{M_i,j} = \left\lfloor \frac{T_{M_i,j}}{T_s} \right\rfloor + 1, \tag{5}$$

where $\lfloor x \rfloor$ denotes the integer part of x. The measured water quantity in M_i will arrive on gate G_j at the date:

$$\Im_{M_i,j} = (k + kd_{M_i,j})T_s. \tag{6}$$

Finally, the transfer time delays between the measurement point M_i and each gate G_j are given by the Management Objective Generation Module and expressed by the vector $\mathbf{T}_{M_i}(n \times 1)$:

$$\mathbf{T}_{M_i} = \left[\Im_{M_i,1},\ldots,\Im_{M_i,j},\ldots,\Im_{M_i,n}\right]^T, \tag{7}$$

where $\Im_{M_i,j}$ is null if $R(i, j) = 0$.

The complex hydrographical network representation, as well as the identification of the transfer time delays, constitutes an essential step for the design of reactive control strategies.

3. Reactive Control Strategy

A reactive control strategy, based on a supervision and hybrid control accommodation framework, is depicted in Figure 3. The hydrographical network is represented by a set of *m* measurement points M_i and n gates G_j locally controlled. For each gate G_j, a weekly objective discharge $q_{j_{obj}}$, and seasonal weights λ_j and μ_j are given by the Management Objective Generation module according to the water contracts and to climatic events. The weekly measurement point objective discharge $Q_{M_{i\,obj}}$ is known.

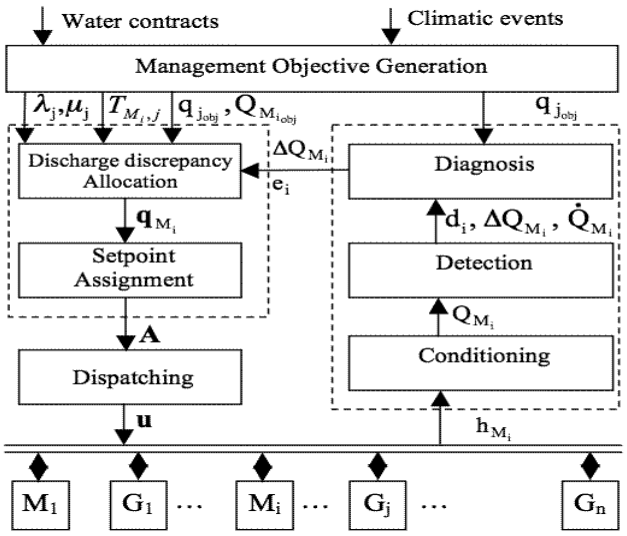

Figure 3. Supervision and hybrid control accommodation framework.

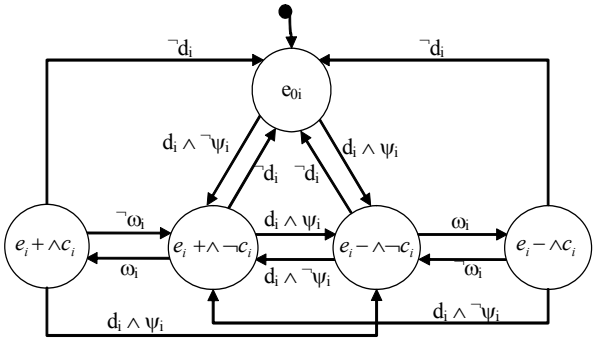

Figure 4. Hybrid automaton for the measurement point M_i.

For each measurement point M_i; i = 1, ..., m, discharge supervision consists in monitoring discharge disturbances and diagnosing the resource state, simultaneously. Limnimeter measurements are conditioned by a low-pass filter on a sliding window that removes wrong data due to transmission errors for instance. Based on the discharge value Q_{M_i} that is measured at each sample time kT_s, detection and diagnosis automata are used respectively to detect a discharge discrepancy and to diagnose the resource states [9]. The concurrent hybrid automaton (*see* Figure 4) is designed for each measurement point M_i. The concurrent hybrid automaton formalism is drawn from the concurrent hybrid automata proposed in [2, 11, 12].

The five pertinent states retained correspond respectively to no-discrepancy state e_0, two states where the discharge discrepancy is either positive (e^+) or negative (e^-) and constant (c_i), and two states where the discharge discrepancy is either positive (e^+) or negative (e^-) and no constant ($\neg c_i$). Transitions between states are defined as conditions on the measured discharge values and variations:

$$\begin{cases} d_i : \left[\left| \Delta Q_{M_i} \right| > th_i \right], \\ \psi_i : \left[\Delta Q_{M_i} < 0 \right], \\ \omega_i : \left[\left| \dot{Q}_{M_i} \right| > dth_i \right], \end{cases} \tag{8}$$

with $\Delta Q_{M_i} = Q_{M_{i\,obj}} - Q_{M_i}$, where Q_{M_i} is the measured discharge, $Q_{M_{i\,obj}}$ is the management objective of the measurement point M_i, $\dot{Q}_{M_i}$ the estimate derivative of Q_{M_i}, th_i and dth_i respectively the detection and diagnosis thresholds.

According to the resource state and the discharge discrepancy ΔQ_{M_i}, the hybrid control accommodation consists in determining the setpoints q_j, and in assigning them to the gates taking into account the hydrographical system dynamics. The resource allocation consists in recalculating setpoints with a goal to route resource in excess to dams and to dispatch amongst the users the resource in lack. At each sample time kT_s, the resource allocation leads to the determination of allocation vector q_{M_i} which is composed of the new computed setpoints. The allocation vector is computed according to the resource state e_i taking into account the seasonal weights λ_j and μ_j.

If the resource state is no diagnose situation (denoted E_0), the setpoints are the objective discharges $q_{j_{obj}}$. The allocation vector is such as:

$$\mathbf{q}_{M_i} = \left[\delta^1_{R(i,1)} q_{1obj}, \ldots, \delta^1_{R(i,j)} q_{j\,obj}, \ldots, \delta^1_{R(i,n)} q_{n\,obj} \right]^T, \tag{9}$$

where n is the total number of gates, and δ^b_a is the Kronecker index.

If the resource state is such as discharge is constant, in lack (denoted $e^- \wedge c_i$) or in excess (denoted $e^+ \wedge c_i$)**,** the water resource is allocated among the gates downstream the measurement point M_i, according to the weights λ_j and μ_j. The allocation strategy consists in optimizing a cost function by linear programming method for each measurement point:

$$f_{M_i} = \sum_{j=1}^{n} \left(\delta^1_{R(i,j)} \chi_{M_{i,j}} \left(q_j - q_{j_{obj}} \right) \right) \tag{10}$$

with $\chi_{M_{i,j}} = \gamma \frac{1}{\lambda_j} + (\gamma - 1) \frac{1}{\mu_j}, \gamma = \frac{1}{2} \left(sign(\Delta Q_{M_i}) + 1 \right)$

The optimization is carried out under constraints:

$$\begin{cases} \sum_{j=1}^{n} \left(R(i,j)(q_j - q_{j_{obj}}) \right) = \Delta Q_{M_i}, \\ q_{j_{\min}} \le q_j \le q_{j_{\max}}, \end{cases} \tag{11}$$

where $q_{j_{\min}}$ and $q_{j_{\max}}$ are respectively the minimum and maximum discharges given by gate, river or canal characteristics. In this case, the allocation vector q_{M_i} is such as:

$$\mathbf{q}_{M_i} = \left[\delta^1_{R(i,1)} q_1, \ldots, \delta^1_{R(i,j)} q_j, \ldots, \delta^1_{R(i,n)} q_n \right]^T, \tag{12}$$

If the resource state is such as discharge is no constant, in lack (denoted $e^- \wedge \neg c_i$) or in excess (denoted $e^+ \wedge \neg c_i$), in order to avoid numerous re-allocation, the water resource is allocated only on one gate,

each one in its turn, at each detection date. The selection of this gate, G_l, is carried out according to the weights λ_j and μ_j, and to a request criterion S_j, storing the gate request and associated to each gate (14). As long as the state is $\neg c_i$, only one gate is assigned but the selected gate changes at each detection date. Because the discrepancy is not constant, at each kT_s, the assigned gate G_l has to absorb only the discrepancy Δq_l^k that was not yet absorbed by the previous ones:

$$\Delta q_l^k = \Delta Q_{M_i}^k - \Delta Q_{M_i}^{k-1}, \tag{13}$$

$$\begin{cases} l \,\middle|\, S_l = \min\limits_{j \in GG_i} S_j, \\ GG_i = \left\{ j \,\middle|\, \begin{array}{ll} j \le n & and \quad R(i,j) = 1 \\ and & q_{j_{\min}} \le q_l^{k-1} + \Delta q_l^k \le q_{j_{\max}} \end{array} \right\}. \end{cases} \tag{14}$$

The allocation vector $\mathbf{q}_{M_i}^k$ is then given by:

$$\begin{cases} \mathbf{q}_{M_i}^k = \left[\delta_{R(i,1)}^1 q_1^{k-1}, \ldots, \delta_{R(i,l)}^1 q_l^k, \ldots, \delta_{R(i,n)}^1 q_n^{k-1} \right]^T, \\ q_l^k = q_l^{k-1} + \Delta q_l^k. \end{cases} \tag{15}$$

At each sample time kT_s, the setpoint assignment matrix $\mathbf{A}_{M_i}^k (H_{M_i} \times n)$, where H_{M_i} is the allocation horizon from M_i (16), is scheduled according to $\mathbf{T}_{M_i}$ and $\mathbf{q}_{M_i}$.

$$H_{M_i} = \max_j T_{M_i}(j). \tag{16}$$

The first row of $\mathbf{A}_{M_i}^k$ contains the setpoints to be assigned to each gate from M_i at the date $(k+1)T_s$, the h^{th} row the ones to be assigned at the date $(k+h)T_s$ following the algorithm given in Table III, the last row the ones to be assigned at the date $(k+H_{M_i})T_s$. At the initial time, the values of the setpoint assignment matrix correspond to the objective discharges, *i.e.* $A_{M_i}^0(h,j) = q_{j_{obj}}$. Then, for h values between the date corresponding to $T_{M_i}(j)$ and the date corresponding to the allocation horizon H_{M_i}, the new computed setpoints $q_{M_i}(j)$ are assigned to $A_{M_i}^k(h,j)$. For values of h such as $T_{M_i}(j)$ is lower than $(k+h)T_s$, the setpoints $q_{M_i}(j)$ are not up-dated, and thus, the values of the setpoint assignment matrix $\mathbf{A}_{M_i}^{k-1}$ at time $(k-1)T_s$, are assigned to the new matrix $\mathbf{A}_{M_i}^k$ at time kT_s, with a shift delay of one period.

TABLE III. Setpoint assignment function of $\mathbf{A}_{M_i}^k$ matrix.

Input: H_{M_i} horizon, $\mathbf{T}_{M_i}$, $\mathbf{q}_{M_i}$ and $\mathbf{A}_{M_i}^{k-1}$ matrices.
Output: $\mathbf{A}_{M_i}^k$ matrix.
For each measurment point M_i
  For each gate G_j
    For each row h of $\mathbf{A}_{M_i}^k$
      If $T_{M_i}(j) \le (k+h)T_s$
        $A_{M_i}^k(h,j) = q_{M_i}(j)$
      Else
        If $h < H_{M_i}$
          $A_{M_i}^k(h,j) = A_{M_i}^{k-1}(h+1,j)$
        Else
          $A_{M_i}^k(h,j) = q_{j_{obj}}$
        EndIf
      EndIf
    EndFor
  EndFor
EndFor

TABLE IV. Assignment function of $\boldsymbol{\alpha}_{M_i}$ matrix.

Input: digraph.
Output: $\boldsymbol{\alpha}_{M_i}$ matrix.
Initialisation of the diagonal of $\boldsymbol{\alpha}_{M_i}$ to 0,
$g \leftarrow$ first gate successor of M_i
Run (M_i, g, $\boldsymbol{\alpha}_{M_i}$)

Run (M_i, g, $\boldsymbol{\alpha}_{M_i}$),
For each successor d of c
  If $L^{c,d}$ is L_S and d is a gate
    Run (M_i, g, $\boldsymbol{\alpha}_{M_i}$)
    $\alpha_{M_i}(d,d) \leftarrow 1$
  EndIf
EndFor

Finally, the setpoints are dispatched with the control period $T_c = \kappa T_s$, where k is an integer. The control setpoint vector denoted $\mathbf{u}$ ($1 \times n$) is updated at each date $k'T_c$, where $k' = \frac{k}{\kappa}$, thanks to the assignment matrix $\mathbf{A}^k_{M_i}$ and the $\boldsymbol{\alpha}_{M_i}$ $(n \times n)$ diagonal control accommodation matrix, with $H = \frac{1}{\kappa}\max_{1 \le i \le m}(H_{M_i})$ the control horizon. For each measurement point M_i, the $\boldsymbol{\alpha}_{M_i}$ matrix, the role of which is to capture the actual influence of the measurement point on the gates, must be determined. In order to generate the $\boldsymbol{\alpha}_{M_i}$ matrix, the weighted digraph (*see* Figure 1.*c* and *d*) is browsed using the algorithm given in table IV, for each measurement point M_i. The control setpoint vector $\mathbf{u}^{k'}$ ($1 \times$ n) is calculated by:

$$u^{k'}(j) = \sum_{i=1}^{m} \alpha_{M_i}(j,j) A^{k'}_{M_i}(1,j). \tag{17}$$

The setpoint dispatching leads to the application of the most recently calculated setpoints. This method increases the control strategy reactivity, because discharge variations between two control dates are taken into account.

4. Management of a Networked Dam-River System

The problem addressed in this section deals with the water asset management of the Purple Dam-River System (PDRS) which is a part of a real networked hydrographical system. The PDRS is characterized by a gridded network configuration with two diffluences and one confluence. The PDRS is composed of the Purple channel upstream reach which supplies the Pink river, the Blue and the Orange channels, the Yellow, Jade and Cyan rivers. The Blue channel supplies the Green, the Red and the Magenta channels and the Indigo river. The Orange channel supplies the Black and the Magenta channels and the Indigo river (*see* Figure 5). The Red channel and Magenta channel supply downstream dams. The channels are composed of several reach sections, *i.e.* a part between two measurement points, about thirty kilometres length. It is considered that all the OCRS of the reach sections have trapezoidal profiles.

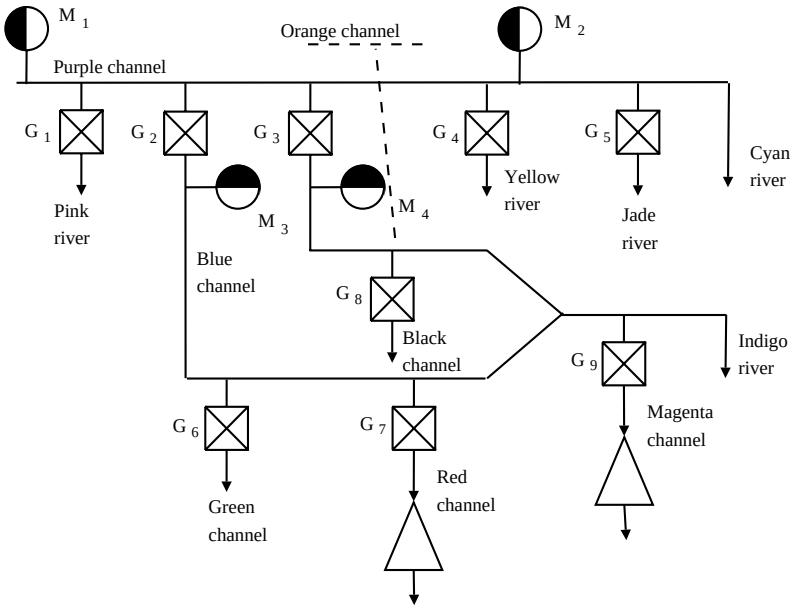

Figure 5. Purple dam-river system.

The PDRS is equipped with telecontrol system to satisfy at best all users and to preserve the resource. The diffluences are equipped at least by a controlled gate and a measurement point. Thus, the discharge flows, downstream the diffluence, are controlled. The PDRS's instrumentation consists of four measurement points M_1 to M_4, and of nine controlled gates G_1 to G_9. The gate characteristics, *i.e.* objective discharge $q_{j_{obj}}$, maximum and minimum discharges $q_{j\max}$ and $q_{j\min}$, and their associated weights λ_j and μ_j, and the objective discharges of the Cyan river and the Indigo river, respectively denoted q_{10} and q_{11}, are given in Table V. The objective discharges of M_1, M_2, M_3 and M_4 correspond, respectively, to 15 m^3/s, 2.5 m^3/s, 5 m^3/s and 2.5 m^3/s.

TABLE V. Gate characteristics**.**

Gate	$q_{j_{obj}}\left[m^3/s\right]$	$q_{j\min}\left[m^3/s\right]$	$q_{j\max}\left[m^3/s\right]$	λ_j	μ_j
G_1	2	0.5	4	4	10
G_2	5	2.5	12	10	4
G_3	2.5	2	8	10	4
G_4	3	1	5	4	10
G_5	1	0.5	3	4	4
G_6	0.5	0.2	2	4	4
G_7	2	1	5	10	4
G_8	1	0.5	3	4	4
G_9	1.5	0.5	7	10	4
q_{10}	1.5	0.5	4	–	–
q_{11}	2.5	1	5	–	–

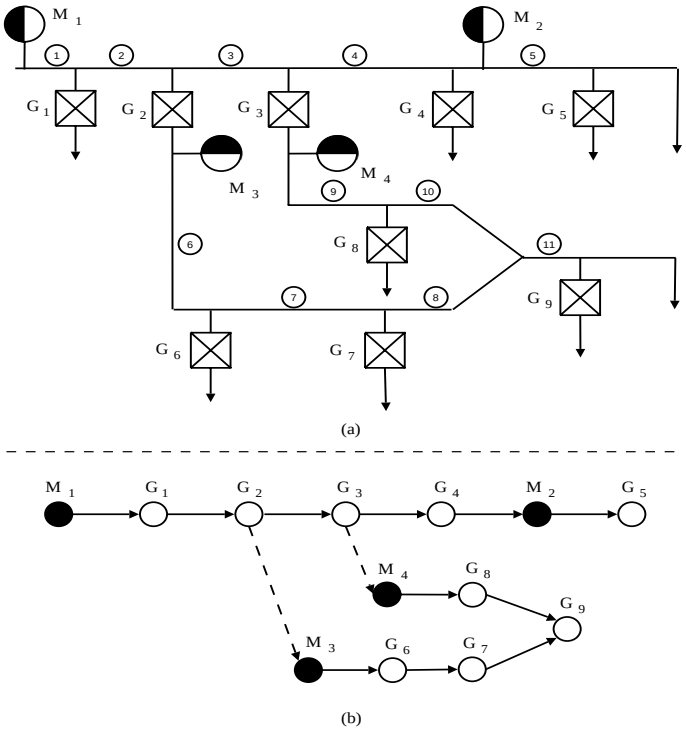

Figure 6. (*a*) PDRS representation, (*b*) its associated digraph representation.

The PDRS is subjected to disturbances upstream the Purple Channel. The considered management scenario consists in:

- Allocating the water quantities in lack, due to withdrawals, amongst the Pink and the Yellow rivers,
- Allocating the water quantities in excess, due to water restitution, toward the Red channel and Magenta channel which supply dams.

Thus, the weights λ_i that are associated to the gates G2, G3, G7 and G9 are the maximum ones (*see* Table V). In addition, the maximum weights μ_i are associated to the gates G_1 and G_4 that correspond to minor priority uses.

The first step of the proposed method is based on the digraph representation of the PDRS, shown in Figure 6, which leads to the determination of the **R** and $\boldsymbol{\alpha}_{M_i}$ matrices according to the algorithms given in Tables I and IV, respectively. The matrix **R** is given by relation (18). The values of $R(1, j)$, *i.e.* from the measurement point M_1 to the gates, is equal to 1 for the gates G_1 to G_5 because there is a direct path between this measurement point and these gates, and 0 otherwise.

$$\mathbf{R} = \begin{bmatrix} 1 & 1 & 1 & 1 & 1 & 0 & 0 & 0 & 0 \\ 0 & 0 & 0 & 0 & 1 & 0 & 0 & 0 & 0 \\ 0 & 0 & 0 & 0 & 0 & 1 & 1 & 0 & 1 \\ 0 & 0 & 0 & 0 & 0 & 0 & 0 & 1 & 1 \end{bmatrix}. \tag{18}$$

The diagonal matrices $\boldsymbol{\alpha}_{M_1}$ to $\boldsymbol{\alpha}_{M_4}$ are given by (19). The fifth value of $\boldsymbol{\alpha}_{M_1}$ is equal to 0 because measurement point M_2 is located upstream gates G_5.

$$\begin{aligned} \boldsymbol{\alpha}_{M_1} &= diag\{1,\ 1,\ 1,\ 1,\ 0,\ 0,\ 0,\ 0,\ 0\}, \\ \boldsymbol{\alpha}_{M_2} &= diag\{0,\ 0,\ 0,\ 0,\ 1,\ 0,\ 0,\ 0,\ 0\}, \\ \boldsymbol{\alpha}_{M_3} &= diag\{0,\ 0,\ 0,\ 0,\ 0,\ 1,\ 1,\ 0,\ 1\}, \\ \boldsymbol{\alpha}_{M_4} &= diag\{0,\ 0,\ 0,\ 0,\ 0,\ 0,\ 0,\ 1,\ 1\}. \end{aligned} \tag{19}$$

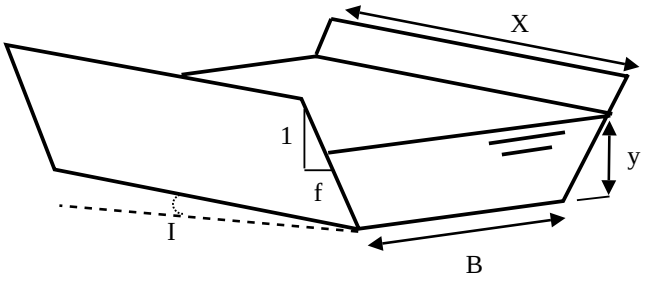

Figure 7. Geometrical characteristics of a trapezoidal profile.

The second step aims at determining the transfer time delays $T_{M_i,j}$. The HYS have been modelled according to the specific length and profile section of each OCRS. The OCRS are numbered from 1 to 11 (*see* Figure 6.a). The OCRS with trapezoidal profile is characterized by the bottom width *B*, the average fruit of the banks *f*, the profile length *X*, the discharge depth *y* and the slope *I* (*see* Figure 7). The geometrical characteristics of the OCRS are given in Table VI.

For trapezoidal profiles, the celerity and diffusion parameters C_e and D_e are expressed as:

$$\begin{cases} C_e = \dfrac{Q_e}{L^2}\left[-f + \dfrac{L}{3}\left(\dfrac{2B}{P_y} + \dfrac{5L}{S} - \dfrac{2}{y}\right)\right] \\ D_e = \dfrac{Q_e}{2LJ}. \end{cases} \tag{20}$$

with $L = B + 2fy$, $S = yB + fy^2$, $P = B + 2y\sqrt{1+f^2}$, and the slope *J* is equivalent to the reach slope *I* for a non critical discharge.

In the studied case, the transfer function is estimated for one operating point for each OCRS. Parameters of the transfer functions identified for reference discharges Q_e, are given in Table VII. The response times *t* are computed from the step response of every identified model, as the time such that 50% of the step response is reached. Then, the transfer delays t_g are computed according to response times *t* and to the PDRS configuration (*see* Figure 8). The measurement points M_2, M_3 and M_4, are located close to their respective upstream gates G_4, G_2 and G_3.

TABLE VI. Geometrical characteristics of the OCRS.

OCRS	B [m]	f	X [m]	I	K
1	5.4	0.8	1200	5.10^{-4}	70
2	5.4	0.95	3700	5.10^{-4}	70
3	5.2	0.95	1500	5.10^{-4}	70
4	5	0.9	2400	5.10^{-4}	70
5	4.8	0.9	1200	5.10^{-4}	70
6	4	0.95	11000	2.10^{-4}	70
7	4	0.95	15000	2.10^{-4}	70
8	4	0.95	2625	4.10^{-4}	70
9	3	0.95	10000	4.10^{-4}	70
10	3	0.95	5000	3.10^{-4}	70
11	3	0.95	2000	2.10^{-4}	70

TABLE VII. Parameters of the transfer functions.

OCRS	$Q_e[m^3/s]$	w_1	w_2	$\tau[s]$	$t[s]$
1	15	570	0	0	395
2	13	1246	0	624	1480
3	8	778	0	69	607
4	5.5	1057	85800	419	1180
5	2.5	673	0	240	707
6	5	7425	10980000	2590	8590
7	4.5	9397	21820000	4540	12400
8	2.5	1619	443200	540	1800
9	2.5	4314	5312000	3970	7710
10	1.5	3610	3149000	1650	4660
11	4	1967	0	0	1360

Finally, the transfer time delays between the measurement points M_i and each gate G_j are expressed according to the sample time T_s (equal to 120 s) using equation (5). The vectors $\mathbf{kd}_{M_i}$ are given by equation (21). Then, at each sample time kT_s, the vectors $\mathbf{T}_{M_i}$ are computed using (6).

$$\begin{aligned}
\mathbf{kd}_{M_1} &= [4,\ 16,\ 21,\ 31,\ 37,\ 0,\ 0,\ 0,\ 0]^T,\\
\mathbf{kd}_{M_2} &= [0,\ 0,\ 0,\ 0,\ 6,\ 0,\ 0,\ 0,\ 0]^T,\\
\mathbf{kd}_{M_3} &= [0,\ 0,\ 0,\ 0,\ 0,\ 72,\ 175,\ 0,\ 201]^T,\\
\mathbf{kd}_{M_4} &= [0,\ 0,\ 0,\ 0,\ 0,\ 0,\ 0,\ 65,\ 115]^T.
\end{aligned} \tag{21}$$

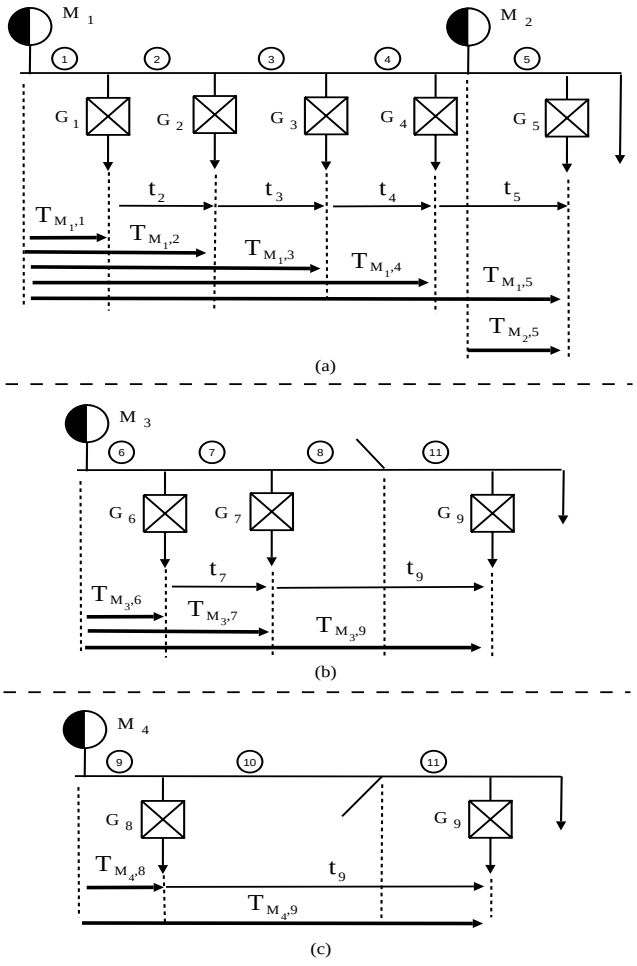

Figure 8. Time delays between measurement points and gates for (*a*) Purple channel stream, (*b*) Blue channel stream, and (*c*) Orange channel stream.

The hydrographical system is subjected to disturbances upstream the measurement points M_1 (*see* Figure 9.*a*). Figure 9 shows discharges measured on M_1, M_3 and M_4, and the discharges q_{10} and q_{11} in the case where no reactive strategy is used (dotted line) and where the reactive strategy is used (continuous line). The results on M_2 and the setpoints dispatched on gates G_5 are not detailed herein.

For each canal reach, Figures 10, 11 and 12 show measured discharges in (*a*), the corresponding resource states diagnosis in (*b*), and the new setpoints that have been dispatched at the gates. As an example, the discharge measured on M_1 is depicted in Figure 10.*a*, the corresponding diagnosed resource state in Figure 10.*b*, the setpoints dispatched on gates G_1, G_2, G_3 and G_4 respectively, in Figures 10.*c*, 10.*d*, 10.*e*, and 10.*f*, and the resource at the end of the channel G_{10} in Figure 10.*g*. The setpoint dispatched on gate G_9 is resulting from the addition of the new setpoints calculated from M_3 and M_4 (*see* Figures 11.*e* and 12.*d*). Thus, in Figure 11.*e*, and in Figure 12.*d*, the setpoint allocated starting from M_3 and, respectively, from M_4 are represented in dashed line, and the resulting setpoint dispatched on gate G_9 in continuous line.

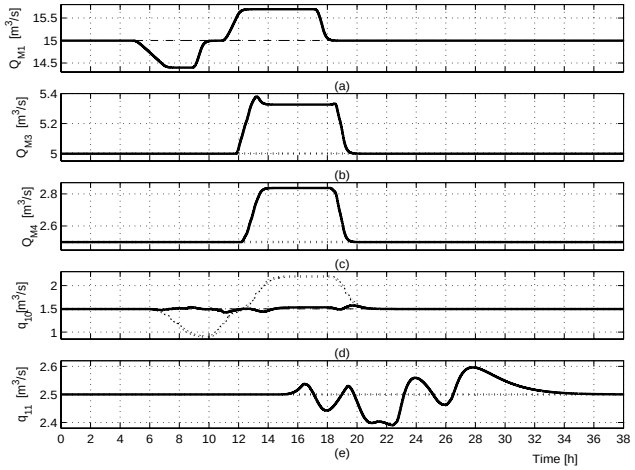

Figure 9. Discharges (*a*) Q_{M_1}, (*b*) Q_{M_3}, (*c*) Q_{M_4}, (*d*) q_{10}, (*e*) q_{11}, with control accommodation (continuous line) and without (dotted line).

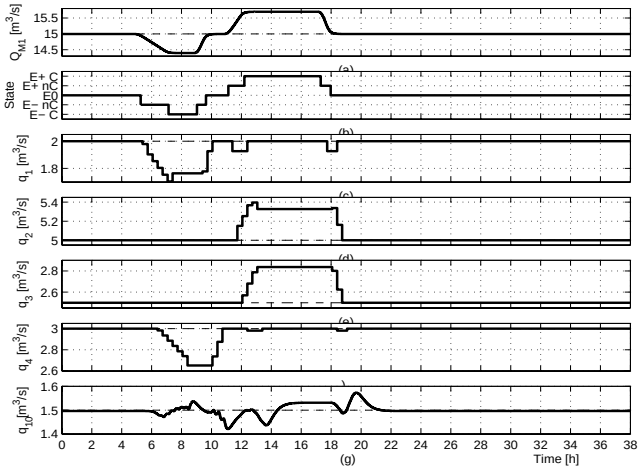

Figure 10. (*a*) Discharge Q_{M_1}, (*b*) diagnosed states from M_1. Setpoints assigned to (*c*) gate G_1, (*d*) gate G_2, (*e*) gate G_3, (*f*) gate G_4, and (*g*) gate G_{10}.

When no strategy is applied, the water quantities in lack or in excess are not allocated on the gates G_1 to G_5 (*see* dotted line in Figure 10.*c*, *d*, *e* and *f*), as shown by the values of the measured discharges on M_3 and M_4 (*see* dotted line in Figure 9.*b* and *c*). The volumes of water due to the disturbances are propagated upstream to downstream on the Purple channel, and the discharge at the end of the channel q_{10} is far from its discharge objective $q_{10_{obj}}$ from the 6^{th} hour to the 20^{th} hour (*see* dotted line in Figure 9.*d*).

When the reactive strategy is applied, as defined by the management scenario, the water quantities in lack are allocated amongst the gates G_1 and G_4 (*see* Figure 10.*c* and *f*), and the water quantities in excess are allocated amongst the gates G_2 and G_3 (*see* Figure 10.*d* and *e*) and finally amongst the gates G_7 and G_9 (*see*

Figures 11.*d*, *e* and 12.*d*). The discharges at the end of the hydrographical system are closed to the objective values, respectively, of 1.5 m^3/s for q_{10} and 2.5 m^3/s for q_{11} (*see* Figure 10.*g* and Figure 11.*f*). The discharge discrepancies at the end of the channels are lower than 0.1 m^3/s. The positive water discrepancy upstream M_1 correspond to a volume of 15000 m^3 during 7 hours. The proposed strategy leads to the allocation of a great part of the water volume measured upstream to M_1 in the downstream dams, by the control of the gates G_2, G_3, G_7 and G_9. A volume of 12000 m^3 is directed from M_1 to the catchment areas, *i.e.* 80 % of the water volume in excess.

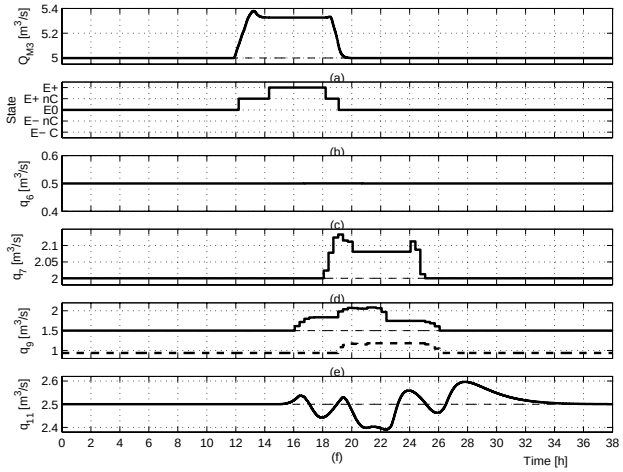

Figure 11. (*a*) Discharge Q_{M_3}, (*b*) diagnosed states from M_3. Setpoints assigned to (*c*) gate G_6, (*d*) gate G_7, (*e*) gate G_9, and (*f*) gate q_{11}.

5. Conclusion

The water-asset management of networked hydrographical systems which are characterized by great dimensions and composed of confluences and equipped diffluences is improved by using the supervision and hybrid control accommodation strategy proposed here. In order to implement the strategy, a weighted digraph representation of dam-river systems was proposed and the resource allocation and setpoint assignment rules were defined. The reactive control strategy aims at detecting discrepancies, diagnosing the resource state and accommodating the discharge setpoints sent to the gates. The strategy was evaluated in the case of a dam-river system composed of two diffluences and one confluence, which supplies with water downstream dams. The simulation results show that the reactive strategy allows valorising the water by resource allocation and setpoint assignment. The strategy proposed in this paper is a generic tool for water resource valorisation whatever the configuration of the dam-river networks is. An interesting extension of the strategy would be the integration of fault detection and isolation methods for sensors and actuators in the supervision scheme.

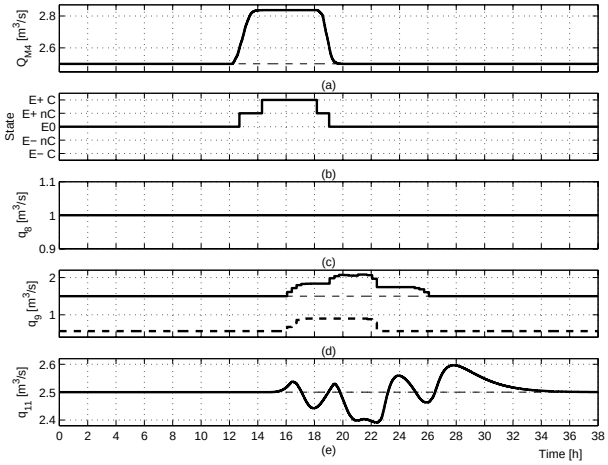

Figure 12. (*a*) Discharge Q_{M_4}, (*b*) diagnosed states from M_4. Setpoints assigned to (*c*) gate G_8, (*d*) gate G_9, and (*e*) gate q_{11}.

REFERENCES

1. ABBOTT, M. and D. BASCO, **Computational Fluid Dynamics: An Introduction for Engineers**, Longman scientific and technical; New York, John Wiley and Son, 1989.

2. BLACKMORE, L., S. FUNIAK, and B. C. WILLIAMS, **A Combinad Stochastic and Greedy Hybrid Estimation Capability for Concurrent Hybrid Models with Autonomous Mode Transitions**, Robotics and Autonomous Systems, Vol. 56, 2008, pp. 105–129.

3. CEMBRANO, G., G. WELLS, J. QUEVEDO, R. PEREZ, and R. ARGELAGUET, **Optial Control of a Water Distribution Network in a Supervisory Control System**, Control Engineering Practice, vol. 8, 2000, pp. 1177–1188.

4. CHAN, C., W. KRITPIPHAT, and P. TONTIWACHWUTHIKUL, **Development of an Intelligent Control System for a Municipal Water Distribution Network**, IEEE Canadian conference on Electrical and Computer Engineering, Vol. 2, 1999, pp. 1108–1113.

5. CHOW, V. T., D. R. MAIDMENT, and L. W. MAYS, **Applied Hydrology**, New York, Paris, McGraw-Hill, 1988.

6. CORMEN, T. H., C. E. LEISERSON, R. L. RIVEST, and C. STEIN, **Introduction to Algorithms**, Second Edition, MIT Press, 2001.

7. DUVIELLA, E., P. CHIRON, and P. CHARBONNAUD, **Hybrid Control Accommodation for Water-asset Management of Hydraulic Systems Subjected to Large Operating Conditions**, ALSIS06, 1st IFAC Workshop on Applications of Large Scale Industrial Systems, Helsinki, Finland, August 30-31, 2006.

8. DUVIELLA, E., P. CHIRON, and P. CHARBONNAUD, **Multimodelling Steps for Free-surface Hydraulic Systems Control**, ICINCO 2006, 3rd International Conference on Informatics in Control, Automation and Robotics, Signal Processing, Systems Modelling and Control, Setubal, Portugal, 1-5 August., 2006.

9. DUVIELLA, E., P. CHIRON, P. CHARBONNAUD, and P. HURAND, **Supervision and Hybrid Control Accommodation for Water Asset Management**, Control Engineering Practice (CEP), Vol. 15, pp. 17–27, 2007.

10. FAYE,R. M., S. SAWADOGO, A. NIANG, and F. MORA-CAMINO, **An Intelligent Decision Support System for Irrigation System Management**, IEEE International Conference on Systems, Man and Cybernetics, SMC'98, October 11-14, San Diego, USA, Vol. 4, 1998, pp. 3908–3913.

11. FUNIAK, S., L. J. BLACKMORE, and B. C. WILLIAMS, **Gaussian Particle Filtering for Concurrent Hybrid Models with Autonomous Transitions**, submitted to Journal of Artificial Intelligence Research, 2004.

12. HOFBAUR, M. W. and B. C. WILLIAMS, **Hybrid Diagnosis with Unknown Behaviorla Modes**, International Workshop on Principles of Diagnosis (Dx-02), Semmering, Austria, May 2-4, pp. 97–105, 2002.

13. ISLAM, A., N. S. RAGHUWANSHI, R. SINGH, and D. J. SEN, **Comparison of Gradually Varied Flow Computation Algorithms for Open-channel Network**, Journal of irrigation and drainage engineering, Vol. 131, No. 5, 2005, pp. 457–465.

14. KUTIJA, V. and C.-J.-M. HEWETT, **Modelling of Supercritical Flow Conditions Revisited; NewC scheme**, Journal of hydraulic research, Vol. 40, No. 2, 2002, pp. 145–152.

15. LISOUNKIN, A., A. SABOV, and G. SCHRECK, **Interpreter Based Model Check for Distribution Networks**, IEEE international conference on industrial informatics, INDIN'O4, 24-26 juin, 2004, pp. 431–435.

16. LITRICO, X. and D. GEORGES, **Robust Continuous-time and Discrete-time Flow Control of a Dam-river System. (i) modeling**, Applied Mathematical Modelling 23, 1999, pp. 809–827.

17. MANSOUR, H. E. F., D. GEORGES, and G. BORNARD, **Optimal Control of Complex Irrigation Systems via Decomposition-Coordination and the Use of Augmented Lagrangian**, IEEE, International Conference on Control Applications, Trieste, Italy, 1998, pp. 3874–3879.

18. NAIDU, B. J., S. M. BHALLAMUDI, and S. NARASIMHAN, **GVF Computation in Tree-type Channel Networks**, Journal of hydraulic engineering, Vol. 123, No. 8, 1997, pp. 700–708.